Chemical Physics Letters 749 (2020) 137446

Contents lists available at ScienceDirect

Chemical Physics Letters

journal homepage: www.elsevier.com/locate/cplett

Research paper

Reaction of N_2O with the prototype singlet biradical CH_2: A theoretical study

Thanh Lam Nguyen[a], A.R. Ravishankara[b], John F. Stanton[a,*]

[a] Quantum Theory Project, Department of Chemistry and Physics, University of Florida, Gainesville, FL 32611, USA
[b] Departments of Chemistry and Atmospheric Sciences, Colorado State University, Ft. Collins, CO 80523, USA[1]

HIGHLIGHTS

- Nitrous oxide is a greenhouse gas and a potential O_3-depleting substance.
- OH, Cl, and NO_3 do not react fast enough with N_2O.
- Mechanism and kinetics of the $^1CH_2 + N_2O$ reaction have been studied for the first time.
- The reaction is very fast with a negative temperature dependence.
- Fast reaction of N_2O with another singlet biradical (e.g. CH_2OO) can be expected.

ABSTRACT

Nitrous oxide (N_2O) is currently the most important ozone-depleting substance emission and is a potent greenhouse gas. It is also a remarkably unreactive chemical species. Any loss processes for N_2O in the troposphere and combustion can be important. Therefore, as part of an effort to investigate how N_2O reacts with prototypical chemical species, its reaction with singlet methylene (CH_2) is studied here using high accuracy thermochemistry mHEAT-345(Q) calculations, together with two-dimensional (E,J) master equation simulations. Two distinct mechanisms (an addition/elimination and an O-abstraction) have been characterized. The reaction is found to be very fast with a negative temperature dependence.

1. Introduction

Laughing gas, nitrous oxide (N_2O), is an important atmospheric species, since it is a strong greenhouse gas, and also destroys (or retards the destruction of ozone through its synergistic influence on halogens) the ozone layer. It is emitted into the atmosphere from both natural and anthropogenic processes [1–4]. N_2O is a very stable species in the troposphere; it reacts extremely slowly with prominent oxidants such as OH, O_3, Cl, and NO_3 [1–3,5,6]. This stability is one of the reasons for its atmospheric importance as a greenhouse gas that accumulates in the atmosphere and is long-enough lived to be transported to the stratosphere. Indeed, the current understanding is that N_2O is predominantly destroyed in the stratosphere, where it can be photolyzed or efficiently react with singlet (^1D) O-atom to yield NO, which then degrades the ozone layer through a nitric oxide (NO) catalytic cycle [1–3].

While natural N_2O emitting sources are governed by the nitrogen cycle, human activity also releases N_2O to the atmosphere. Indeed, it is estimated that the majority of current increased emissions is due to human activities, and out of that, roughly 15% is due to combustion [2].

In previous papers [5,6], we have reported theoretical studies for the reactions of N_2O with OH and NO_3; these two reactions were found to be too slow to be detected experimentally [5,6]. Here we study the potential reaction of N_2O with singlet CH_2, a reaction that can occur in combustion processes where both N_2O and CH_2 could be present. In this work, we report a theoretical study of the reaction mechanism and chemical kinetics of the oxidation of N_2O by singlet CH_2. We also expect that a study of reaction of N_2O with CH_2 may provide insights into how N_2O will react with other biradical species.

2. Methodology

2.1. Quantum chemical calculations

For the [CH_2N_2O] reaction system, full HEAT calculations [7–9] are demanding, so a pragmatic model is desirable. In this work, a

* Corresponding author.
E-mail address: johnstanton@ufl.edu (J.F. Stanton).
[1] Also associated with the Le Studium, Advanced Institute for Research, Loire Valley, Orleans, France.

https://doi.org/10.1016/j.cplett.2020.137446
Received 5 March 2020; Received in revised form 1 April 2020; Accepted 2 April 2020
Available online 03 April 2020
0009-2614/

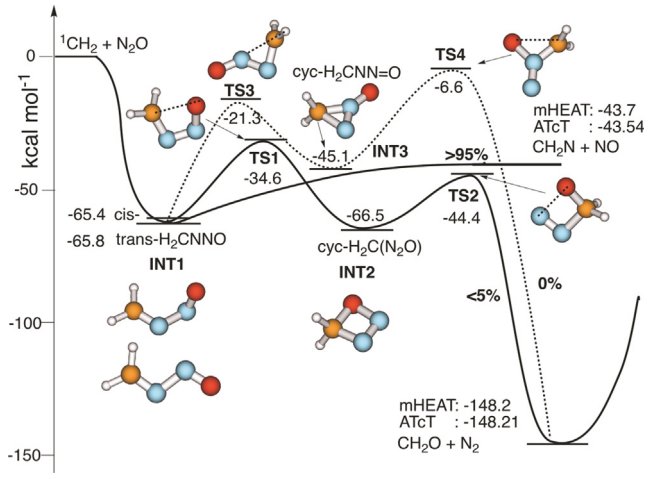

Fig. 1. A Schematic of the reaction energy profile for the addition/elimination mechanism in the N_2O + $^1CH_2$ reaction calculated with mHEAT-345(Q) method. Where possible, the benchmark reaction enthalpies from ATcT [12] are given for comparison. The dashed line indicates a path not taken in the reaction while the solid line is the one suggested for the reaction. The major product is suggested to be CH_2N + NO.

modification of the method known as HEAT-345(Q) (designated hereafter as mHEAT-345(Q)) [10], which has previously been applied to medium-sized molecules [11], was used. The mHEAT-345(Q) is a composite method in which the energy is given as a sum of separately evaluated contributions [10]:

$$E_{mHEAT} = E^{\infty}_{SCF} + \Delta E^{\infty}_{CCSD(T)} + \Delta E_{T-(T)} + \Delta E_{(Q)-T} + \Delta E_{core} + \Delta E_{ZPE} + \Delta E_{DBOC} + \Delta E_{Scalar} + \Delta E_{SO} \quad (1)$$

where E^{∞}_{SCF} is the Hartree-Fock energy, $\Delta E^{\infty}_{CCSD(T)}$ is the electron correlation energy calculated in the frozen-core approximation with the CCSD(T) method, $\Delta E_{T-(T)}$ is the different energy of CCSDT and CCSD(T) calculations, $\Delta E_{(Q)-T}$ is the different energy of CCSDT(Q) and CCSDT calculations, ΔE_{core} is the core correlation correction, ΔE_{ZPE} is the anharmonic zero-point vibrational energy, ΔE_{DBOC} is the diagonal Born-Oppenheimer correction, ΔE_{Scalar} is the scalar relativistic effect, and ΔE_{SO} is the spin-orbit correction.

Further details of mHEAT have been documented elsewhere [10]. As seen in Fig. 1, mHEAT calculations yield accuracies better than 0.5 kcal/mol (as compared to benchmark ATcT values) [12] for the two reaction enthalpies; comparable accuracy can be expected for other species. All calculations were done using the CFOUR quantum chemistry package [13]. The thermochemistry of the pathways for the reaction of N_2O and singlet CH_2 (the potential energy surface) has previously been reported using a lower level of theory, QCISD(T)/6-311G(d,p)//B3LYP/6-31G(d,p) [14]. Herein, we report not only the potential energy surface calculated using higher level of theory (better accuracy) but also explore the associated chemical kinetics.

2.2. Two-dimensional master equation approach

The mHEAT calculations mentioned above provide structures, energies, rovibrational parameters, and anharmonic constants for relevant stationary points. These data are then used as input to the fixed-J two-dimensional master equation (fj-2DME) [11,15–17] – which depends on both internal energy and total angular momentum – to obtain thermal rate coefficients (as well as product yields) as functions of temperature and pressure. The fj-2DME has been used in previous works, and the method has recently been benchmarked by comparing it to full E,J-resolved 2DME calculations [11,15–17]. The **TS** code, which uses a steady-state approach to solve a fj-2DME for a chemically activated reaction system (and now available in the MULTIWELL software package [18]) was used for this purpose. N_2 is used as the bath gas, with collisional parameters of σ = 3.7047 Å and ε/k_B = 84.942 K [18]. Collisional data for the [CH_2N_2O] system are not available; so those for n-butane, whose size is similar to that of [CH_2N_2O], were used: σ = 5.40 Å and ε/k_B = 307 K [18]. A single exponential function was chosen to model downward energy transfer process (P_d). The average amount of energy transferred per collision in a deactivation event is given empirically by:

$$\langle \Delta E \rangle_d = 200 \times \left(\frac{T}{298}\right)^{0.8} \text{ in } \text{cm}^{-1}, \quad \text{where T is the reaction temperature in K} \quad (2)$$

A probability function of energy transfer (P_u) in the upward direction can then be obtained from considerations of detailed balance:

$$P_u \times F^B_u = P_d \times F^B_d \quad (3)$$

where F^B is the Boltzmann thermal energy distribution function of an activated intermediate calculated at the reaction temperature T.

In the fj-2DME, the maximum (ceiling) energy is chosen to be 40,000 cm^{-1} relative to the lowest-lying intermediate, which allows us to treat the wide range of reaction temperatures considered here. An energy grained bin of 10 cm^{-1} is used. The same bin size of 10 cm^{-1} is also applied to compute anharmonic vibrational densities and sums of states for minima and tight transition structures (TS), respectively, using the BDENS [19] and SCTST [20–23] codes of MULTIWELL, which automatically include coupled vibrations and multi-dimensional quantum mechanical tunneling corrections. For a variational (loose) TS (e.g. a barrierless reaction path), variational RRKM theory [24,25] is used to characterize the kinetic bottleneck.

All stationary points on the potential energy surface are approximated by a symmetric top, of which rotational energy levels are given by Eq. (4):

$$E_r(J,K) = J(J+1)\bar{B} + (A-\bar{B})K^2, \quad \text{with } \bar{B} = \sqrt{B \cdot C} \text{ and } -J \le K \le +J \quad (4)$$

where J is the total rotational angular momentum quantum number, K is the quantum number that represents the portion of the total angular momentum that lies along the unique rotational axis. A, B, and C are rotational constants.

While total angular momentum J is always conserved, its projection (K) is not. Therefore, the convolution of external rotational quantum states with vibrational quantum states depends on how K is treated: either "*active*" or "*adiabatic*" [26–28]. Assuming that K is active for both TS and reactant, the rovibrational density (ρ_{rv}) and sum (G_{rv}) of states can be obtained using Eq. (5) (the J-shifting approximation):

$$G_{rv}(E,J) = \sum_{K=-J}^{K=+J} G_v(E - E_r(J,K))$$
$$\rho_{rv}(E,J) = \sum_{K=-J}^{K=+J} \rho_v(E - E_r(J,K)) \quad (5)$$

where ρ_v and G_v is the anharmonic (coupled) vibrational density and sum of states, respectively.

In addition, the **TS** code of MULTIWELL requires a capture rate coefficient (k_c(T)) for the association step of N_2O with CH_2 (without a barrier) to form an initial energized adduct at each temperature. k_c(T) can be calculated variationally at the high-pressure limit using Eq. (6):

$$k_c(T) = \frac{\sigma}{h} \times \frac{Q^{\neq}_{tr} Q^{\neq}_{e}}{Q^{re}_{CH_2} \bullet Q^{re}_{N_2O}} \times \sum_{J=0}^{\infty} (2J+1) \int_0^{\infty} \text{Min}[G^{\neq}_{rv}(E,J)] \times \exp(-E/k_B T) dE \quad (6)$$

where h is Planck's constant, k_B is Boltzmann's constant, and σ is the

reaction path degeneracy. $Q^{re}_{CH_2}$ and $Q^{re}_{N_2O}$ are the complete partition functions for CH_2 and N_2O, respectively. Q_{tr} is the translational partition function, and Q_e is the electronic partition function (the superscripts "re" and "≠" designate reactants and transition state, respectively). All electronic partition functions of singlet CH_2, N_2O, and all stationary points are equal to 1 for a singlet electronic state. It should be mentioned that triplet methylene ($^3CH_2$) is about 9 kcal/mol more stable than $^1CH_2$, but an electronic partition function of $^3CH_2$ is not included in the calculations because we focus on the singlet electronic state PESs only. There may be surface hopping between singlet and triplet PESs, but such effects are not included here, as a principle point of this work is to study the reaction of N_2O with a singlet biradical. The rate coefficient for product formation is finally computed using Eq. (7):

$$k_P(T) = \gamma_P \cdot k_c(T) \quad (7)$$

γ_P above is the product yield, which is calculated as a function of both temperature and pressure using the **TS** code.

3. Results and discussion

3.1. Reaction mechanisms

The interaction of singlet CH_2 with N_2O can take place via two different pathways: one is the addition/elimination mechanism displayed in Fig. 1, and the other is an O-abstraction shown in Fig. 2.

As seen in Fig. 1, singlet CH_2 can add to the terminal N-atom of N_2O (without a barrier) leading to the formation of **INT1**, H_2CNNO. This association can produce both the trans- and cis-conformation **INT1** in vibrationally excited states with an internal energy of *ca.* 65.5 kcal/mol. Trans is about 0.4 kcal/mol more stable and can rapidly interconvert to cis through a low barrier; hence, they are treated as a single species in the kinetics analysis. When **INT1** is formed, it prefers to undergo decomposition to yield various products rather than dissociate back to the initial reactants, simply because the barrier heights to decomposition lie below the entrance channel. Starting at **INT1**, there are three distinct pathways to dissociation: (i) first, the N—N bond in **INT1** can be broken without a kinetic barrier to give CH_2N and NO; (ii) second, **INT1** can undergo ring closure via TS1 leading to four-membered ring structure **INT2**, which subsequently dissociates via TS2 to yield the very stable $CH_2O + N_2$ products; (iii) third, **INT1** can isomerize via TS3 to a three membered-ring configuration **INT3**, which then dissociates (via TS4) to the same products as (ii). However, it is obvious that the third pathway

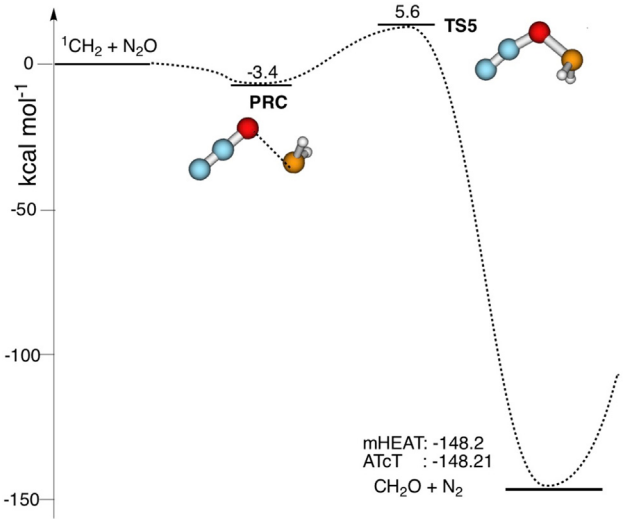

Fig. 2. A Schematic of the reaction energy profile for the O-abstraction mechanism in the $N_2O + {}^1CH_2$ reaction calculated with mHEAT-345(Q) method. Where possible, the benchmark reaction enthalpies from ATcT [12] are given for comparison.

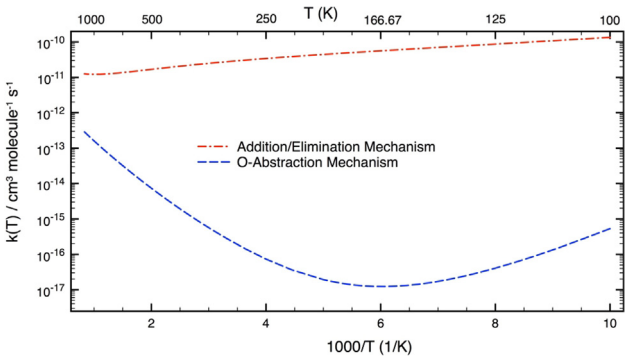

Fig. 3. Individual rate coefficients for the addition/elimination and the O-abstraction pathway in the $N_2O + {}^1CH_2$ reaction, calculated as a function of temperature.

is unimportant because it involves a higher barrier.

Fig. 2 shows the O-abstraction mechanism through a pre-reactive van der Waals complex **PRC**, which has a binding energy of about 3.4 kcal/mol. **PRC** can then undergo either O-abstraction via a tight TS5 to yield $CH_2O + N_2$ or redissociation via a loose, variational TS back to initial reactants. The latter step is obviously dominant because it requires less energy and has a looser TS.

3.2. Chemical kinetics calculations

Because the two reaction mechanisms mentioned above are uncoupled, kinetics analyses for them can be done separately. A comparison between the two can be made by using rate coefficients calculated at 100–1000 K as shown in Fig. 3. Both reaction pathways are found to be (nearly) pressure-independent for $P < 10$ atm. It is obvious that the addition/elimination mechanism is favored while the O-abstraction mechanism could play a minor role at (very high) combustion temperatures; for example, at T = 1000 K, the contribution of the O-abstraction pathway is still less than 5% of the overall reaction.

For the O-abstraction pathway, Fig. 3 also shows a complicated temperature dependence of the calculated rate coefficient: in the low temperature regime, it decreases with increasing temperature and reaches a minimum near 165 K; then, at higher temperatures, it increases with temperature. This behavior can be explained as follows: quantum mechanical tunneling is very important at low temperatures, thus causing a negative temperature dependence, even for the motion of oxygen atom in this scenario. However, tunneling effects decrease sharply as temperature increases, ultimately becoming insignificant at high temperatures (see Fig. S1 in the Supplementary Material). As a result, the reaction has a positive (normal) temperature dependence at temperatures relative to both the atmosphere and combustion. The same characteristics were seen in other reactions reported earlier [29,30].

For the addition/elimination pathway, all dissociating TSs lie well below the initial reactants, which means that the reaction rate coefficient is governed by the association step of N_2O and CH_2, a barrierless process. Thus, its dependence on temperature is negative: reducing from *ca.* 10^{-10} cm^3/s at 100 K to *ca.* 10^{-11} cm^3/s at 1000 K (see Fig. 3). Moreover, it is found that the addition/elimination pathway yields $CH_2N + NO$ as major products (> 95%) and $CH_2O + N_2$ as minor products (< 5%); that is, the kinetically-favored products are not the thermally-favored products. These product branching ratios depend very slightly on temperature. Taking the contribution of the O-abstraction pathway into account, overall product yields can be estimated as 90 ± 5% for $CH_2N + NO$ with the balance going to $CH_2O + N_2$.

It may be worth mentioning that a singlet species can normally undergo insertion into a single-bond of its co-reactant (e.g. O (^1D) + $CH_4 \rightarrow CH_3OH$). However, N_2O (N≡N═O) does not have a

single bond. In addition, our calculations also show that stable singlet adducts (i.e. both $^1NCH_2NO$ and $^1NNCH_2O$, which are expected to be formed) do not exist. Thus, we conclude that an insertion pathway is not operative in this reaction.

It is also important to evaluate the possible impact of triplet methylene reaction, given that both singlet and triplet methylene can be produced in combustion environments. A theoretical study [31] previously reported a barrier of (at least) about 15 kcal/mol for the reaction of $^3CH_2$ and N_2O [31]. Therefore, the triplet methylene reaction is negligibly slow in the atmosphere, but may play a (minor) role in high temperature combustion. Because the $^1CH_2 + N_2O$ reaction produces singlet intermediates, which have a high internal energy and quickly decompose to products, the surface hopping from the singlet to triplet PES is likely have a small probability and cannot compete with the spin-conserved process on the singlet surface. In contrast, because of the high barrier, the $^3CH_2 + N_2O$ reaction occurs slowly, thus it has a sufficient time to undergo an ISC process from the triplet to singlet PES. So, the impact of the triplet methylene reaction is expected to be unimportant.

4. Conclusions

We have studied the reaction of singlet CH_2 with N_2O using high accuracy thermochemistry mHEAT-345(Q) calculations, followed by two-dimensional master equation simulations to predict product yields and rate coefficients. Two distinctive mechanisms including an addition/elimination (major) and an O-abstraction (minor) pathway have been characterized. The calculated results show that the reaction is very fast with a negative temperature dependence: decreasing from about 10^{-10} cm^3/s at 100 K to about 10^{-11} cm^3/s at 1000 K. In addition, the predicted reaction products are: 90 ± 5% for $CH_2N + NO$ and 10 ± 5% for $CH_2O + N_2$, which are almost pressure- and temperature-independent.

We have shown that N_2O reacts very efficiently with CH_2 and it does so via an initial end-on collision. This is an important finding for a few reasons. Like the atmospherically important analogous reaction with O(^1D), the reaction studied here is between N_2O and a (prototypical) singlet "biradical". Unlike the case of O(^1D), this singlet does not directly insert into the N=N or N−O bond, but rather proceeds via an end-on attack. Such a pathway may well be common, and suggests that singlet biradical species in the troposphere (notably Criegee intermediates) might also react similarly with N_2O. We will study this latter process in future work.

5. Credit author statement

All authors have significantly equal contributions to this work.

Declaration of Competing Interest

The authors declare that they have no known competing financial interests or personal relationships that could have appeared to influence the work reported in this paper.

Acknowledgements

Work at the University of Florida was supported by the U.S. National Science Foundation (Grant CHE-1664325) and Department of Energy, Office of Science, Office of Basic Energy Sciences under Award DE-FG02-07ER15884. Work of ARR was supported by Colorado State University and Le Studium Advanced Institute for Research, Loire Valley, Orleans, France.

Appendix A. Supplementary material

Theoretical methods, optimized geometries, and rovibrational parameters for various stationary points are provided. Supplementary data to this article can be found online at https://doi.org/10.1016/j.cplett.2020.137446.

References

[1] A.R. Ravishankara, J.S. Daniel, R.W. Portmann, Nitrous Oxide (N_2O): The dominant ozone-depleting substance emitted in the 21st century, Science 326 (2009) 123–125.
[2] Drawing down N2O to protect climate and the ozone layer. A UNEP synthesis report. United Nations Enviroment Programme (UNEP), Nairobi, Kenya, United Nations Environment Programme (UNEP), Nairobi, Kenya, 2013.
[3] D. Kanter, D.L. Mauzerall, A.R. Ravishankara, J.S. Daniel, R.W. Portmann, P.M. Grabiel, W.R. Moomaw, J.N. Galloway, A post-Kyoto partner: Considering the stratospheric ozone regime as a tool to manage nitrous oxide (vol 110, pg 4451, 2013), Proc. Natl. Acad. Sci. USA 110 (2013) 16693–16693.
[4] R.L. Thompson, L. Lassaletta, P.K. Patra, C. Wilson, K.C. Wells, A. Gressent, E.N. Koffi, M.P. Chipperfield, W. Winiwarter, E.A. Davidson, H. Tian, J.G. Canadell, Acceleration of global N_2O emissions seen from two decades of atmospheric inversion, Nat. Clim. Change 9 (2019) 993–+.
[5] T.L. Nguyen, M.N. Romanias, A.R. Ravishankara, A.M. Zaras, P. Dagaut, J.F. Stanton, The atmospheric impact of the reaction of N_2O with NO_3: A theoretical study, Chem. Phys. Lett. 731 (2019).
[6] T.L. Nguyen, A.R. Ravishankara, J.F. Stanton, Analysis of the potential atmospheric impact of the reaction of N_2O with OH, Chem. Phys. Lett. 708 (2018) 100–105.
[7] A. Tajti, P.G. Szalay, A.G. Csaszar, M. Kallay, J. Gauss, E.F. Valeev, B.A. Flowers, J. Vazquez, J.F. Stanton, HEAT: High accuracy extrapolated ab initio thermochemistry, J. Chem. Phys. 121 (2004) 11599–11613.
[8] Y.J. Bomble, J. Vazquez, M. Kallay, C. Michauk, P.G. Szalay, A.G. Csaszar, J. Gauss, J.F. Stanton, High-accuracy extrapolated ab initio thermochemistry. II. Minor improvements to the protocol and a vital simplification, J. Chem. Phys. 125 (2006).
[9] M.E. Harding, J. Vazquez, B. Ruscic, A.K. Wilson, J. Gauss, J.F. Stanton, High-accuracy extrapolated ab initio thermochemistry. III. Additional improvements and overview, J. Chem. Phys. 128 (2008).
[10] J.H. Thorpe, C.A. Lopez, T.L. Nguyen, J.H. Baraban, D.H. Bross, B. Ruscic, J.F. Stanton, High-accuracy extrapolated ab initio thermochemistry. IV. A modified recipe for computational efficiency, J. Chem. Phys. 150 (2019).
[11] T.L. Nguyen, L. McCaslin, M.C. McCarthy, J.F. Stanton, Communication: Thermal unimolecular decomposition of syn-CH_3CHOO: A kinetic study, J. Chem. Phys. 145 (2016) 131102.
[12] B. Ruscic, D.H. Bross, Active Thermochemical Tables (ATcT) values based on ver. 1.122d of the Thermochemical Network (2018), available at ATcT.anl.gov, 2018.
[13] J.F. Stanton et al., CFOUR, a quantum chemical program package, For the current version, see http://www.cfour.de.
[14] J.J. Liu, J.K. Feng, Y.H. Ding, A.M. Ren, S.F. Wang, C.C. Sun, F.A. Kong, Theoretical study on the potential energy surface of the $^1CH_2 + N_2O$ reaction, J. Phys. Chem. A 105 (2001) 5885–5895.
[15] T.L. Nguyen, H. Lee, D.A. Matthews, M.C. McCarthy, J.F. Stanton, Stabilization of the simplest criegee intermediate from the reaction between ozone and ethylene: A high-level quantum chemical and kinetic analysis of ozonolysis, J. Phys. Chem. A 119 (2015) 5524–5533.
[16] T.L. Nguyen, J.F. Stanton, A steady-state approximation to the two-dimensional master equation for chemical kinetics calculations, J. Phys. Chem. A 119 (2015) 7627–7636.
[17] T.L. Nguyen, J.H. Thorpe, D.H. Bross, B. Ruscic, J.F. Stanton, Unimolecular reaction of methyl isocyanide to acetonitrile: a high-level theoretical study, J. Phys. Chem. Lett. 9 (2018) 2532–2538.
[18] J.R. Barker, T.L. Nguyen, J.F. Stanton, C. Aieta, M. Ceotto, F. Gabas, T.J.D. Kumar, C.G.L. Li, L.L. Lohr, A. Maranzana, N.F. Ortiz, J.M. Preses, J.M. Simmie, J.A. Sonk, P.J. Stimac, MULTIWELL Program Suite, Climate and Space Sciences and Engineering, University of Michigan, Ann Arbor, MI 48109-2143, May 2017.
[19] T.L. Nguyen, J.R. Barker, Sums and densities of fully coupled anharmonic vibrational states: a comparison of three practical methods, J. Phys. Chem. A 114 (2010) 3718–3730.
[20] T.L. Nguyen, J.F. Stanton, J.R. Barker, A practical implementation of semi-classical transition state theory for polyatomics, Chem. Phys. Lett. 499 (2010) 9–15.
[21] W.H. Miller, Semiclassical theory for non-separable systems – construction of good action-angle variables for reaction-rate constants, Faraday Discuss. 62 (1977) 40–46.
[22] W.H. Miller, R. Hernandez, N.C. Handy, D. Jayatilaka, A. Willetts, Ab initio calculation of anharmonic constants for a transition-state, with application to semiclassical transition-state tunneling probabilities, Chem. Phys. Lett. 172 (1990) 62–68.
[23] R. Hernandez, W.H. Miller, Semiclassical transition-state theory – a new perspective, Chem. Phys. Lett. 214 (1993) 129–136.
[24] W.L. Hase, Variational unimolecular rate theory, Acc. Chem. Res. 16 (1983) 258–264.
[25] D.G. Truhlar, B.C. Garrett, Variational transition-state theory, Annu. Rev. Phys. Chem. 35 (1984) 159–189.
[26] L. Zhu, W.L. Hase, Comparison of models for calculating the Rrkm unimolecular

rate constant-K(E, J), Chem. Phys. Lett. 175 (1990) 117–124.
[27] E.E. Aubanel, D.M. Wardlaw, L. Zhu, W.L. Hase, Role of angular-momentum in statistical unimolecular rate theory, Int. Rev. Phys. Chem. 10 (1991) 249–286.
[28] L. Zhu, W. Chen, W.L. Hase, E.W. Kaiser, Comparison of models for treating angular-momentum in Rrkm calculations with vibrator transition-states – pressure and temperature-dependence of $Cl + C_2H_2$ association, J. Phys. Chem.-Us 97 (1993) 311–322.
[29] T.L. Nguyen, J.F. Stanton, Ab initio thermal rate calculations of HO + HO = $O(^3P)$ + H_2O reaction and isotopologues, J. Phys. Chem. A 117 (2013) 2678–2686.
[30] T.L. Nguyen, B. Ruscic, J.F. Stanton, A master equation simulation for the OH + CH_3OH reaction, J. Chem. Phys. 150 (2019).
[31] J.J. Liu, Y.H. Ding, J.K. Feng, Y.G. Tao, C.C. Sun, Theoretical study on mechanism of the $^3CH_2$ + N_2O reaction, J. Phys. Chem. A 106 (2002) 1746–1764.